Ultrawideband VNA Based Channel Sounding System for Centimetre and Millimetre Wave Bands

Hejselbæk, Johannes; Fan, Wei; Pedersen, Gert F.

Published in:
Personal, Indoor, and Mobile Radio Communications (PIMRC), 2016 IEEE 27th Annual International Symposium on

DOI (link to publication from Publisher):
10.1109/PIMRC.2016.7794728

Publication date:
2016

Document Version
Accepted author manuscript, peer reviewed version

Ultrawideband VNA Based Channel Sounding System for Centimetre and Millimetre Wave Bands

Johannes Hejselbaek, Wei Fan and Gert F. Pedersen
Department of Electronic Systems, Faculty of Engineering and Science, Aalborg University, Denmark
Email: {joh, wfa, gf}@es.aau.dk

***Abstract*—Channel characterization of multipath channels at centimetre and millimetre wave bands is of interest from both academia and industry, especially for the frequency bands that are under consideration for 5G mobile communication systems. In this paper, we first demonstrate the limitations of an existing vector network analyzer (VNA) based channel sounding system in terms of frequency range and measurement range. After that, an improved system is proposed to address these limitations. The proposed system is capable of measuring from 2 to 50 GHz at 30 meters distances. A measurement campaign utilizing the proposed setup equipped with rotational directive horn antennas, with a focus on multi-band power-angle-delay profiles, was performed. The measured frequency bands are 18 - 20 GHz, 25 - 27 GHz, 28 - 30 GHz and 38 - 40 GHz.**

***Index Terms*—centimetre and millimetre wave bands, multi-path channels, 5G mobile communication, multi-band angular power spectrum measurements.**

I. Introduction

The increasing growth in demand for mobile data drives the industry towards a fifth-generation mobile network (5G) [1]. To facilitate the demand for higher data rates, there is a need for unused radio spectrum. The super-high-frequency (SHF) bands (3 – 30 GHz) and the extremely high-frequency (EHF) bands (30 – 300 GHz), also referred to as centimetre- and millimetre-wave bands have the potential to provide the needed bandwidth [2].

To enable the system design for the 5G mobile network, understanding of the propagation channels is essential [3], [4]. One of the important channel characteristics is the Angle-of-Arrivals (AoAs) of multipath channels. The possible utilization of high frequency for 5G systems enables the implementation of massive antenna arrays due to the small antenna element. This enables 5G systems to excessively utilize the spatial dimension via e.g., beamforming algorithms, which can boost the system performance significantly in terms of data rate and signal strength levels [5], [6]. Therefore, knowledge of the AoAs of the propagation environments is the focus of this paper.

Channel characterization above 6 GHz for various propagation environments has attracted huge research attention in recent years. To ensure the realism of the modelled propagation channels, many measurement campaigns were carried out for various bands above 6 GHz. For the unlicensed frequency band at 60 GHz, used for IEEE 802.11ad, there are significant available studies [7], [8]. The 60 GHz system is mainly for short range indoor to indoor communication due to the high path-loss introduced by oxygen absorption. For longer range systems, e.g. the potential 5G cellular systems, lower bands are suggested [3], [9], [10]. More specifically, there is an interest in the 28 - 30 GHz band, where some experimental measurements have been conducted [11]–[14].

In the literature, there are mainly two types of channel sounding systems [15]. The first, known as direct pulse measurements, utilizes a dedicated correlative channel sounder and operates in time-domain and the other, known as swept frequency measurements, utilizes a Vector Network Analyser (VNA) based system, and it operates in frequency-domain. The correlative channel sounders are capable of recovering an estimate of the channel impulse response (CIR) very fast [16]. This is an advantage for collecting large datasets for time-variant scenarios. However, the complexity of generating the sounding pulse poses limitations to the obtainable bandwidth of these systems [17]. A VNA based system do not have this limitation as it sweeps the chosen frequency band while the channel frequency response is measured between two ports of the VNA. This allows for very large bandwidths to be measured and hence it is a popular method especially for Ultrawideband (UWB) applications [18], [19].

Large bandwidths are expected for the future 5G mobile communication system, which encourages the use of a VNA for measurements. As it is difficult to assess the possible frequency bands over which the mm-wave systems are expected to operate at this stage, various frequency bands above 6 GHz are proposed and under investigation. Therefore, it is beneficial to record the channel over the whole interested band and understand the frequency dependence of channel parameters scenarios for future mm-Wave systems. This knowledge would help operators decide which frequency bands are preferable and how to utilize the channels best at different frequency bands. The VNA based channel sounding system is often adopted for mm-Wave channel measurements, due to high cost and complexity of the dedicated channel sounder [15], [17]. However, there are some well-known limitations with the VNA system. The measurement system is limited in range (i.e. distance between transmitter (TX) and receiver (RX)), especially for mm-Wave systems. TX/RX signals are carried via RF cables, which introduce a power loss. Furthermore, the measurement scenario should be static as it takes time for VNA system to sweep over frequency domain for multiple locations. Hence, channel sounding using a VNA is normally used for short range indoor scenarios [15].

VNA based channel sounding systems have been extensively used for low-band (below 6GHz) and high-band (above 6GHz) in the literature. For frequencies below 6 GHz, there are publications addressing the measurement range issue. In [20], a system capable of supporting a TX-RX separation of up to 45 meters was presented. A system utilizing optics for extending the range up to 100 meters is presented in [18] for frequency below 6GHz as well. In [21], the measurement range up to 1000 meters was demonstrated with two synchronized VNAs. For systems operating above 6 GHz, most of the proposals are for systems operating at 60 GHz and therefore not intended for longer range measurements. A system operating at 26 GHz sweeping a 5 GHz bandwidth (24 to 29 GHz) is presented in [22]. However, this system is only operated in a range of 5 meters. In [23] a system operating at 28 GHz is presented which have a range of 7 meters, but only sweeping 1 GHz (27.5 - 28.5 GHz). The same frequency and bandwidth are used for the system presented in [24], where the range is here 30 meters. For larger bandwidths used in multi-band measurements, a system is presented in [14], [25], [26]. This has a limited range of about 10 meters and is restricted in which frequency bands it can measure, 2 - 4 GHz, 14 - 16 GHz and 28 - 30 GHz. This paper presents the cause of these limitations and a proposal for an improved measurement setup with an extended frequency range and also capable of extending the operational range.

This paper is organized as follows. Section II describes the existing VNA-based channel sounding system and presents the limitations of the system. This is followed by a presentation of the proposed new measurement system and its capabilities. Section III presents new multi-band power-angle-delay measurements. Section IV summarizes this work.

II. Channel Sounding System

To extend the physical range of measurements conducted using a VNA, the VNA is used together with mixers. The basic principle is that via down-converting the signals with a mixer, the cable loss, which is the main limiting factor for measurement range, can be reduced.

A. Limitations of Existing System

The existing system presented in [14], [25], [26] is based on a mixer solution from Agilent. This solution is consisting of the following three elements:

- Distribution unit for the local oscillator and intermediate frequency.
- Reference mixer.
- Test mixer.

The distribution unit is in principle just an amplifier and splitter of the LO (Local Oscillator) from the VNA (PNA) to the mixers, as depicted in Fig. 1. It also provides amplification of the IF (Intermediate Frequency) from the mixers along with demultiplexing of the IF from the test mixer.

The purpose of both the test mixer and reference mixer is to down-convert the received high-frequency signal to IF. The main difference between the test mixer and the reference mixer is that the test mixer multiplexes the IF on the LO resulting in only one cable having to go from distribution unit to mixer. The reference mixer uses separate lines for the LO and IF and also provides feedback for the ALC (Automatic Level Control) in the distribution unit. Using the reference mixer enables the system to utilize leveled output power.

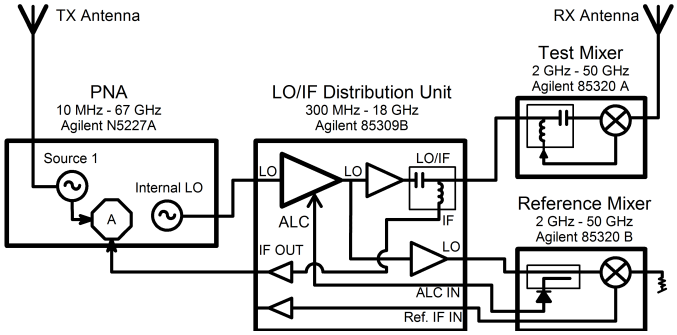

Fig. 1. Block diagram of the existing measurement system.

A measurement is conducted to test the stability of the system. In this test the TX port is connected directly to the test mixer input. Following the manufacturer specified warm up period a normalization/calibration is performed. This procedure sets the trace to zero in the chosen frequency span from 2 GHz to 30 GHz (1001 points). The VNA was set to continuous sweeping, while the drift from the normalization is recorded. The drift after 10 sweeps is shown in Fig. 2. It is clear that power variations exist, especially for frequency band from 2-6 GHz and 18-26.5 GHz. The lower band at 2-6 GHz shows deviations up to 1 dB and the higher band at 18-26.5 GHz shows deviations up to 3 dB. Below, these deviations in the measurement system are investigated.

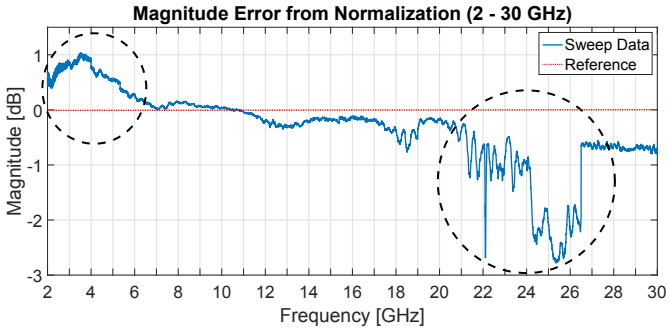

Fig. 2. Deviation from the normalization/calibration curve for the frequency sweep from 2 to 30 GHz using the existing system.

As shown in Fig. 1, the internal LO output from the PNA is ported to the distribution unit. This setting was chosen as it was the most straightforward way to use and did not require any additional setup of the PNA. However, by measuring the output of the internal LO, it became evident that it only utilizes the fundamental frequency up to 26.5 GHz before it switches to operate on 3rd harmonics of the frequency. This is

problematic, as the amplifiers in the distribution unit only have a frequency range from 300 MHz to 18 GHz. As a result, the required amplification of the LO from 18 to 26.5 GHz does not exist, which results in large power variations within 18-26.5 GHz, as shown in Fig. 2.

The power variations within 2-6 GHz were found to be a result of to high LO power at the test mixer, for the lower frequencies. The purpose of the reference mixer is to control the LO power levels by using the ALC to compensate the frequency dependent loss of the cable connecting the mixers to the distribution unit. In the existing VNA system, two cables of different types and lengths are used to connect between the distribution unit and the two mixers. As a result, the ALC did not function as intended for the low band.

B. Proposed Improvement of Existing System

As discussed in Section A., the existing measurement system in general had two problems:

1) Over-powering at lower frequencies
2) Under-powering at higher frequencies

To address the under-powering at higher frequencies, an alternative source for the LO has to be used. The PNA is equipped with two source oscillators (signal generators), as depicted in Fig. 3. The two oscillators are locked to each other, but it is possible to introduce a frequency offset between them. In the proposed setup, one oscillator is connected to the TX antenna (source 1), while the other oscillator (source 2) is used as LO and set to operate on a lower harmonic of the desired frequency. For example, source 1 can be set to sweep from 2 GHz to 30 GHz, while source 2 can sweep from 2/3 GHz to 10 GHz, using the 3rd harmonics. This ensures that the system operates within the frequency limits of the amplifiers of the distribution unit. The lowered frequency also reduces the cable losses which can improve the operational range of the system. It could be tempting to lower the LO frequency further by using higher harmonics. However, using harmonics have the cost of the sensitivity of the mixers and using higher harmonics will decrease the sensitivity level further.

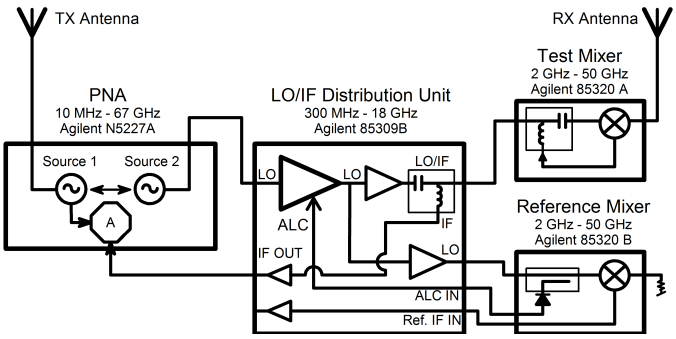

Fig. 3. Block diagram of the proposed measurement system.

As seen in Fig. 3, the reference mixer is terminated at its input. Even though it is not needed to use a long cable for the reference mixer, this is a solution to address the over-powering at lower frequencies. By using the same type and length of cabling to the reference mixer as for the test mixer, it is possible for the ALC to provide the same LO power over the selected frequency band.

Using the same settings as for the sweep shown in Fig. 2, a sweep with the proposed solutions is conducted. The resulting magnitude error is shown in Fig. 4. A significant improvement is achieved in terms of power variations. The only significant variations are seen close to 2.5 GHz, which is due to the settling time of the ALC. This settling time introduces a variation of up to 0.5 dB at the low frequency, aside from this a variation of less than 0.1 dB is seen.

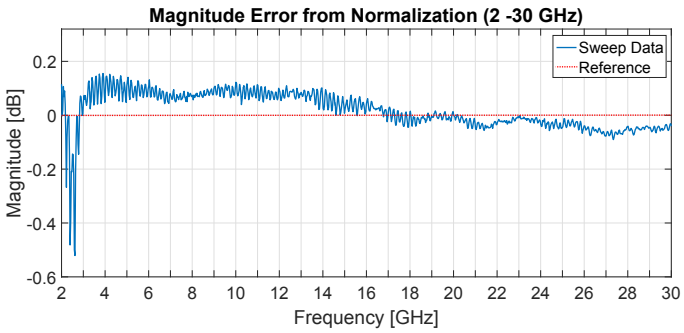

Fig. 4. Deviation from the normalization/calibration curve for the frequency sweep from 2 to 30 GHz using the proposed system.

C. Improved System Capability

With the proposed systems, the measurement system capability in terms of measurement range and frequency range can be greatly improved. The frequency range of the used mixers is 2 to 50 GHz, which becomes the limiting factor as the PNA have a larger span. The measurement range is limited by the link budget. Below, the system link budget is discussed separately for the RF chain and in-the-air propagation loss.

The sensitivity level for the test mixer sets the limit for the lowest detectable power at its RF input. When operating the test mixers with 3rd harmonic, the sensitivity level for RF input is -118 dBm for 2 GHz to 18 GHz, -103 dBm for 18 GHz to 40 GHz and -100 dBm for 40 GHz to 50 GHz, respectively. This is on the condition that the LO input power at the mixer is at +12 to +17 dBm. To investigate the link budget of the RF chain, the most critical frequency 50 GHz is selected, as an example for measurement range. As discussed earlier, 3rd harmonics (i.e. 16.67 GHz) would be utilized for 50 GHz. According to the specifications, the maximum LO output power from the distribution unit is +23.5 dBm in the frequency range from 6.2 to 18 GHz when given an input signal at +6 dBm. This leaves $23.5 - 12 = 11.5$ dB for cable loss between distribution unit and mixer as illustrated in Fig. 5.

The PNA is capable of delivering +18 dBm (@16.5 GHz), leaving 12 dB for cable loss between PNA and distribution unit. The used LO cable has a loss of 0.78 dB/m (@16.5 GHz), giving that at least $^{12}/_{0.78} = 15.3$ m can be used for the cable from PNA to distribution unit and $^{11.5}/_{0.78} = 14.7$ m of cable

can be used from the distribution unit to the test mixer. In total, this gives an operational range of 30 meters when measuring at 50 GHz. When measuring at lower frequencies, the LO frequency will also be lower, allowing for longer cables to be used. As an example, the operational range is 41 meters when measuring at 30 GHz. The range of the LO distribution system could be extended by introducing further amplification.

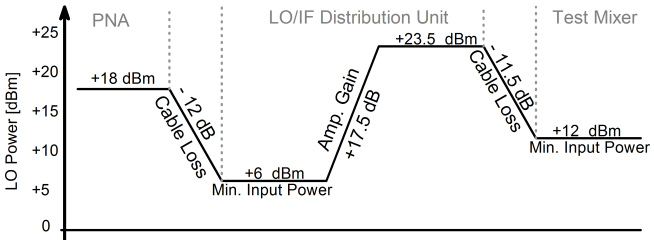

Fig. 5. Link-budget for the LO power distribution.

Additional to the RF chain loss, the signals also suffer from in-the-air propagation loss. The path loss, however, highly depends on the measurement scenario, e.g. Line-Of-Sight (LOS) or Non-LOS, together with the frequency measured. For the proposed measurement system, the maximum leveled output power from source 1 when sweeping up to 50 GHz is 9 dBm. The sensitivity of the test mixer is -100 dBm, which gives a maximum path loss of 109 dB. Using Friis free space propagation loss for LOS scenario and assuming 0 dB TX/RX antenna gains, the maximum transmission range is 32.6 meters for 50 GHz. If sweeping to a maximum of 30 GHz the leveled output power can be increased to 12 dBm while the sensitivity level of the test mixer is lowered to -103 dBm. This gives that the range will be 34.6 meters in same LOS scenario for 30 GHz. The transmission range can be further improved utilizing high gain antennas.

III. Angular Power Measurement using New Proposed System

Using the presented measurement system, a multi-band measurement has been conducted aiming at capturing the power-angle-delay profiles. The selected measured bands are 18 - 20 GHz, 25 - 27 GHz, 28 - 30 GHz and 38 - 40 GHz. The chosen bands are based on the candidates for future 5G frequency allocations presented in [9].

A. Measurement Setup

Two frequency sweeps from 18 to 27 GHz and from 28 to 40 GHz, utilizing two standard gain horn antennas for RX were performed. As the TX antenna, the biconical antenna presented in [27] is used. All the antennas used are vertically polarized. The properties of the used antennas are presented in TABLE I.

Both of the frequency sweeps from 18 to 27 GHz and from 28 to 40 GHz are recorded using 10001 frequency points. The four bands of interest all have a bandwidth of 2 GHz, giving a delay resolution of 0.5 ns equivalent to a spatial resolution of 0.15 m.

TABLE I
Properties for the used antennas

Antenna Type	**Freq. Range** [GHz]	**HPBW, Azimuth** [^{o}]	**Gain** [dB]
Biconical (1.5 - 42 GHz)	18 - 20	Omni	4.5
	25 - 27	Omni	4.8
	28 - 30	Omni	4.6
	38 - 40	Omni	3.7
Horn (18 - 27 GHz)	18 - 20	21.5	18.7
	25 - 27	15.7	21.2
Horn (27 - 40 GHz)	28 - 30	21,2	18.8
	38 - 40	15.8	21.1

Two different scenarios were studied in a rich furnished laboratory as shown in Fig. 6. The first is an LOS scenario, shown left in Fig. 6. The second, shown right in Fig. 6, is a obstructed line-of-sight (O-LOS) scenario, where the LOS path is blocked by an obstruction. The O-LOS scenario was created by placing a cubicle divider in the direct path between TX and RX at a distance of 4.15 m from the TX. The distance between TX and RX is 8 m for both scenarios.

Fig. 6. Measurement scenario. Left in the figure the LOS case is shown and right in the figure the O-LOS case is shown. The biconical TX antenna, seen in the bottom of both scenarios, is encased in styrofoam as a part of its design.

The TX power for all the measurements is 9 dBm. When starting the measurement the orientation of the RX horn antennas is 90^o of bore-sight of the TX antenna. It is then rotated clockwise in 1^o steps between each sweep for a full 360^o measurement.

B. Measurement Results

The power-angle-delay profiles for the four measured bands presented in Fig. 7 - 10, are obtained via an inverse Fourier transformation of the frequency sweeps for each orientation. To suppress the effect of side lobes, a Hamming window has been applied to the data. The frequency response of the used

antennas has not been removed from the recorded frequency sweeps and thus are embedded in the presented plots. The dynamic range of the plots is set to 40 dB. The four measured bands are presented for both the LOS and O-LOS scenario. The same power scale is used to enable comparison between the scenarios.

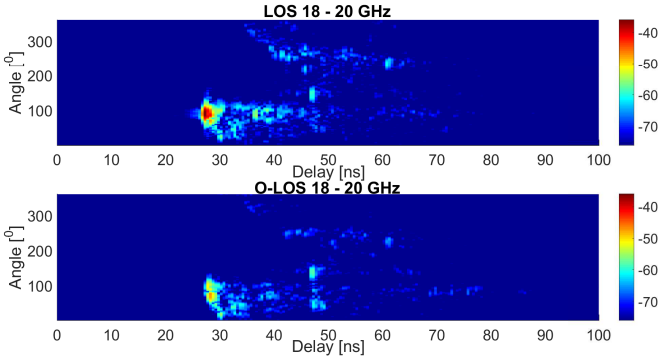

Fig. 7. Power-angle-delay profile measured using a directional horn antenna for 18 - 20 GHz in LOS and O-LOS.

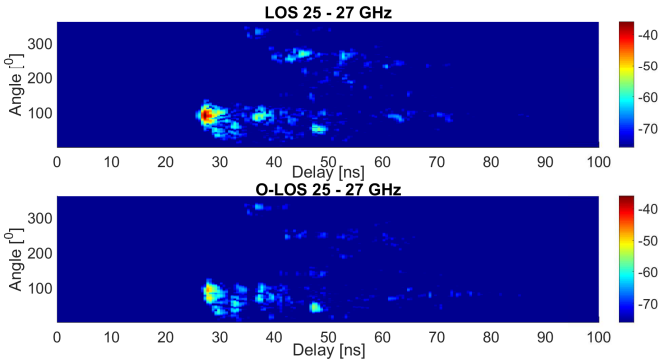

Fig. 8. Power-angle-delay profile measured using a directional horn antenna for 25 - 27 GHz in LOS and O-LOS.

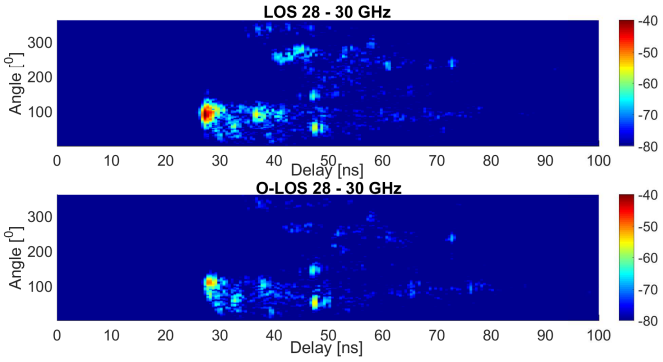

Fig. 9. Power-angle-delay profile measured using a directional horn antenna for 28 - 30 GHz in LOS and O-LOS.

In Fig. 7 - 10, the dominant path is at 90^o, which corresponds to the LOS path between the TX and RX. The delay of the dominant path, for the LOS scenario, is 27 ns corresponding to 8.1 m in accordance with the distance between TX and RX in the chosen scenario. The delay of the dominant path for the O-LOS is 28 ns which are only 1 ns longer than for the LOS scenario. This indicates that it might be a diffraction around the edges of the obstruction. The power difference between the dominant path in LOS and O-LOS is around 9 dB, varying with only 0.5 dB between the four bands.

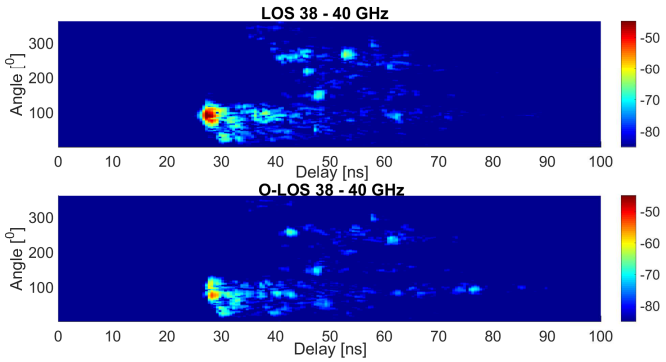

Fig. 10. Power-angle-delay profile measured using a directional horn antenna for 38 - 40 GHz in LOS and O-LOS.

The number of multipath components is similar for all four bands, given the chosen dynamic range. In addition, some similarity in the location of the components can be observed in the four bands. There is a tendency for the components to be located around 90^o and 270^o. The components at 270^o are presumed to be backscatters from the wall behind the RX, as seen from the TX. It can be seen in Fig. 10 that the component arriving at 55 ns from 270^o in the LOS scenario diminishes in the O-LOS scenario. This is due to the lower power of the dominant path, which results in a very low power of the backscatter.

A comparison of the omnidirectional power delay profile for the measured bands is presented in Fig. 11. To enable comparison of the slope of the delay profiles, the maximum power of the LOS component have been used for normalization of each band separately. The O-LOS profiles have been normalized using the same value as for the LOS.

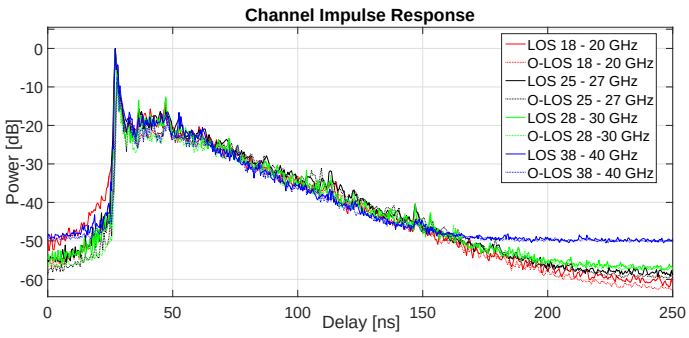

Fig. 11. Channel impulse response for the measured bands in both LOS and O-LOS.

An interesting finding from Fig. 11 is that all four bands in both LOS and O-LOS scenario present the same decay slope

from 50 to 150 ns. In [14], it was concluded that the decay rate is independent of frequency. However, the measurements were performed in an empty basement scenario and therefore the impact of furniture in the room is not investigated. In this paper, we demonstrated that the decay rate is frequency independent for a rich furnished laboratory.

IV. Conclusion

This work presents the improvement of an existing VNA based measurement system contributing with a wider frequency range and longer measurement range. The proposed system is capable of measuring from 2 to 50 GHz with a power drift of less than 0.5 dB in the whole span. The range of the system has been extended to 30 meters for measurement at 50 GHz and even further for measurement at lower frequencies.

Multi-band measurements in both LOS and O-LOS have been conducted using the proposed system Measurements. The conducted measurements showed that the frequency bands 18 - 20 GHz, 25 - 27 GHz, 28 - 30 GHz and 38 - 40 GHz have similar power-angle-delay properties. Another interesting result is the similarity in the slope of the delay decay slope for all measured bands.

Acknowledgment

The work have been conducted under the framework of the VIRTUOSO project. The Danish National Advanced Technology Foundation supports this project together with industry partners. The authors would like to thank Kim Olesen and Anders Karstensen for assistance with measurements.

References

[1] P. Demestichas, A. Georgakopoulos, D. Karvounas, K. Tsagkaris, V. Stavroulaki, J. Lu, C. Xiong, and J. Yao, "5g on the horizon: Key challenges for the radio-access network," *Vehicular Technology Magazine, IEEE*, vol. 8, no. 3, pp. 47–53, Sept 2013.

[2] Q. Li, H. Niu, A. Papathanassiou, and G. Wu, "5g network capacity: Key elements and technologies," *Vehicular Technology Magazine, IEEE*, vol. 9, no. 1, pp. 71–78, March 2014.

[3] L. Wei, R. Q. Hu, Y. Qian, and G. Wu, "Key elements to enable millimeter wave communications for 5g wireless systems," *IEEE Wireless Communications*, vol. 21, no. 6, pp. 136–143, December 2014.

[4] Y. Kim, H. Y. Lee, P. Hwang, R. K. Patro, J. Lee, W. Roh, and K. Cheun, "Feasibility of mobile cellular communications at millimeter wave frequency," *IEEE Journal of Selected Topics in Signal Processing*, vol. PP, no. 99, pp. 1–1, 2016.

[5] W. Roh, J.-Y. Seol, J. Park, B. Lee, J. Lee, Y. Kim, J. Cho, K. Cheun, and F. Aryanfar, "Millimeter-wave beamforming as an enabling technology for 5g cellular communications: theoretical feasibility and prototype results," *Communications Magazine, IEEE*, vol. 52, no. 2, pp. 106–113, February 2014.

[6] S. Han, C. l. I, Z. Xu, and C. Rowell, "Large-scale antenna systems with hybrid analog and digital beamforming for millimeter wave 5g," *IEEE Communications Magazine*, vol. 53, no. 1, pp. 186–194, January 2015.

[7] A. Maltsev, R. Maslennikov, A. Sevastyanov, A. Khoryaev, and A. Lomayev, "Experimental investigations of 60 ghz wlan systems in office environment," *Selected Areas in Communications, IEEE Journal on*, vol. 27, no. 8, pp. 1488–1499, October 2009.

[8] W. Fu, J. Hu, and S. Zhang, "Frequency-domain measurement of 60 ghz indoor channels: a measurement setup, literature data, and analysis," *IEEE Instrumentation Measurement Magazine*, vol. 16, no. 2, pp. 34–40, April 2013.

[9] Ofcom, "Spectrum above 6 ghz for future mobile communications," Ofcom UK, Riverside House, 2a Southwark Bridge Road, London, Consultation Report, 2015.

[10] S. Methley, W. Webb, S. Walker, and J. Parker, "Study on the suitability of potential candidate frequency bands above 6ghz for future 5g mobile broadband systems," Quotient Associates Limited, Compass House, Vision Park, Chivers Way Histon, Cambridge, CB24 9AD, UK, Technical Report, 2015.

[11] S. Rangan, T. Rappaport, and E. Erkip, "Millimeter-wave cellular wireless networks: Potentials and challenges," *Proceedings of the IEEE*, vol. 102, no. 3, pp. 366–385, March 2014.

[12] T. Rappaport, S. Sun, R. Mayzus, H. Zhao, Y. Azar, K. Wang, G. Wong, J. Schulz, M. Samimi, and F. Gutierrez, "Millimeter wave mobile communications for 5g cellular: It will work!" *Access, IEEE*, vol. 1, pp. 335–349, 2013.

[13] T. Rappaport, F. Gutierrez, E. Ben-Dor, J. Murdock, Y. Qiao, and J. Tamir, "Broadband millimeter-wave propagation measurements and models using adaptive-beam antennas for outdoor urban cellular communications," *Antennas and Propagation, IEEE Transactions on*, vol. 61, no. 4, pp. 1850–1859, April 2013.

[14] W. Fan, I. C. Llorente, J. Ødum Nielsen, K. Olesen, and G. F. Pedersen, "Measured wideband characteristics of indoor channels at centimetric and millimetric bands," *EURASIP Journal on Wireless Communications and Networking*, vol. Pre Press, no. Special issue on Radio Channel models for higher frequency bands, 2016.

[15] A. F. Molisch, *Wireless communications*. IEEE Press, 2005, iSBN: 978-0-470-84888-3.

[16] J. Ødum Nielsen, J. B. Andersen, P. C. F. Eggers, G. F. Pedersen, K. Olesen, E. H. Sørensen, and H. Suda, "Measurements of indoor 16x32 wideband mimo channels at 5.8 ghz," in *Proceedings of the 2004 International Symposium on Spread Spectrum Techniques and Applications*, May 2004.

[17] A. F. Molisch, "Ultrawideband propagation channels-theory, measurement, and modeling," *IEEE Transactions on Vehicular Technology*, vol. 54, no. 5, pp. 1528–1545, Sept 2005.

[18] A. M. Street, L. Lukama, and D. J. Edwards, "Use of vnas for wideband propagation measurements," *IEE Proceedings - Communications*, vol. 148, no. 6, pp. 411–415, Dec 2001.

[19] S. Ranvier, M. Kyro, K. Haneda, T. Mustonen, C. Icheln, and P. Vainikainen, "Vna-based wideband 60 ghz mimo channel sounder with 3-d arrays," in *Radio and Wireless Symposium, 2009. RWS '09. IEEE*, Jan 2009, pp. 308–311.

[20] S. S. Ghassemzadeh, R. Jana, C. W. Rice, W. Turin, and V. Tarokh, "A statistical path loss model for in-home uwb channels," in *Ultra Wideband Systems and Technologies, 2002. Digest of Papers. 2002 IEEE Conference on*, May 2002, pp. 59–64.

[21] K. Sarabandi, N. Behdad, A. Nashashibi, M. Casciato, L. Pierce, and F. Wang, "A measurement system for ultrawide-band communication channel characterization," *IEEE Transactions on Antennas and Propagation*, vol. 53, no. 7, pp. 2146–2155, July 2005.

[22] Y. Rikuta, S. Fujita, F. Ohkubo, H. Hosoya, K. Hamaguchi, J. i. Takada, and T. Kobayashi, "Indoor channel measurement of 26 ghz band uwb communication system," in *Ultra-Wideband, The 2006 IEEE 2006 International Conference on*, Sept 2006, pp. 219–224.

[23] X. Wu, Y. Zhang, C. X. Wang, G. Goussetis, e. H. M. Aggoune, and M. M. Alwakeel, "28 ghz indoor channel measurements and modelling in laboratory environment using directional antennas," in *2015 9th European Conference on Antennas and Propagation (EuCAP)*, May 2015, pp. 1–5.

[24] M. Lei, J. Zhang, T. Lei, and D. Du, "28-ghz indoor channel measurements and analysis of propagation characteristics," in *Personal, Indoor, and Mobile Radio Communication (PIMRC), 2014 IEEE 25th Annual International Symposium on*, Sept 2014, pp. 208–212.

[25] W. Fan, I. C. Llorente, and G. F. Pedersen, "Comparative study of centimetric and millimetric propagation channels in indoor environments," in *2016 10th European Conference on Antennas and Propagation (EuCAP 2016)*, April 2016.

[26] A. Karstensen, W. Fan, I. C. Llorente, and G. F. Pedersen, "Comparison of ray tracing simulations and channel measurements at mmwave bands for indoor scenarios," in *2016 10th European Conference on Antennas and Propagation (EuCAP 2016)*, April 2016.

[27] S. S. Zhekov, A. Tatomirescu, and G. F. Pedersen, "Modified biconical antenna for ultrawideband applications," in *2016 10th European Conference on Antennas and Propagation (EuCAP 2016)*, April 2016.